PERGAMON

Planetary and Space Science 49 (2001) 107–114

Planetary and Space Science

www.elsevier.nl/locate/planspasci

Generation of electron-acoustic waves in the magnetosphere

S.V. Singh *, G.S. Lakhina

Indian Institute of Geomagnetism, Dr. Nanabhai Moos Marg, Colaba, Mumbai-400005, India

Received 21 October 1999; received in revised form 25 May 2000; accepted 11 July 2000

Abstract

Generation of electron-acoustic waves (EAWs) is examined in an unmagnetized, four-component plasma consisting of stationary cold and hot Maxwellian electrons, drifting electron beam and ions. The addition of hot background electrons to the previously existing three-component model reduces the excited EAW frequencies and growth rates. Electrostatic linear dispersion equation is solved analytically for the growth rate and real frequency. The linear theory of EAWs is applied to the dayside auroral zone and other regions of the magnetosphere. The mechanism can generate frequencies over a wide range of 5 Hz–6 kHz, 3 Hz–4 kHz and 5 Hz–6 kHz in the dayside auroral zone, plasma sheet boundary layer and polar cusp, respectively. The e-folding time of the instability is of the order of a few milliseconds, and the waves are expected to grow nonlinearly to large amplitudes. Our four-component model can explain the broadband electrostatic noise (BEN) observations below the total electron plasma frequencies in these regions fairly well.

1. Introduction

Satellite measurements have established the presence of broadband electrostatic wave emissions in various regions of the Earth's magnetosphere. The frequency range of the emissions extends from few Hz, up to and well above the electron plasma frequency. These emissions are known as broadband electrostatic noise (BEN). BEN has been observed in magnetotail, bow shock, polar cusp and auroral region of the earth's magnetosphere and has been associated with different modes of the plasma. BEN was first observed in the magnetotail by *IMP* 7 and 8 satellites (Scarf et al., 1974; Gurnett et al., 1976) and later on by *ISEE* satellite (Cattell et al., 1986) in frequency range extending from 10 Hz to 1 kHz and with intensities ranging from 50 μV/m to 5 mV/m. Due to its broad range of frequency, it was suggested that several wave modes may be contributing to BEN. Various researchers have tried to explain BEN generation in terms of ion-acoustic and ion-cyclotron waves (Gurnett et al., 1976; Gurnett and Frank, 1977), lower hybrid drift waves (Huba et al., 1978), ion-beam driven modes (Grabbe and Eastman, 1984; Omidi, 1985; Akimoto and Omidi, 1986; Ashour-Abdalla and Okuda, 1986; Shriver and Ashour-Abdalla, 1987), velocity shear instabilities (Lakhina, 1987), electron plasma oscillations (Parks et al., 1984; Baumjohann et al., 1989), and field-aligned current-driven modes (Shriver and Ashour-Abdalla, 1989).

Observations have shown the presence of ion and electron beams in the plasma sheet boundary layer (PSBL) and their association with the BEN emissions. Thus, several studies were undertaken based on ion-beam-driven modes in this region. While low and middle frequency part of the BEN can be explained by these modes, high-frequency part could not be reproduced. In order to explain high-frequency BEN by ion-beam-generated modes, Grabbe (1985) found that the addition of cold electron component to the model raises the frequency of unstable waves closer to electron plasma frequency. Later on, Shriver and Ashour-Abdalla (1987) examined the ion-beam driven modes with additional cold electron component and identified them as electron-acoustic modes. It was also suggested that high-frequency part of the BEN can be explained by Doppler shifted ion- and electron-acoustic waves. Field-aligned electron beams and bi-directional electron pitch angle anisotropies have also been detected in PSBL (Hada et al., 1981; Parks et al., 1984; Onsager et al., 1990). Parks et al., (1984) demonstrated that large amplitude BEN occurred in a layer adjacent to the plasma sheet and contained parallel and anti-parallel electron beams, density gradient and earthward streaming ions. Cold electron-beam-driven electrostatic waves were studied by Shriver and Ashour-Abdalla (1989) with hot background of electrons through computer simulations and also theoretically. The low-frequency part of wave spectra was found to

* Corresponding author.
E-mail address: satyavir@iig.iigm.res.in (S.V. Singh).

0032-0633/01/$ - see front matter
PII: S0032-0633(00)00126-4

be dominated by ion-acoustic waves, and the high-frequency part by electron-acoustic waves. Simulation results showed that the free energy source for these instabilities is destroyed rapidly resulting in the heating of the background plasma. Later on, Onsager et al. (1993) suggested that high frequency, broadband electrostatic waves may be generated by unstable electron distributions in the PSBL.

In the auroral region, the intense electric field noise along the auroral field lines was first detected by $OVO-1$ spacecraft (Heppner, 1969) and later on by $DE-1$ (Gurnett et al., 1976) and *Hawkeye* 1 and *IMP* 6 (Gurnett and Frank, 1977) satellites. High time resolution observations by Swedish satellite *Viking* revealed the presence of BEN in the low-density auroral regimes at an altitude of 2000 –10,000 km. The total electric field of BEN in this region can reach up to 100 mV/m. The low-frequency BEN is more intense than the high-frequency BEN. Also, BEN emissions in the dayside and nightside auroral regions differ quantitatively as well as in temporal structures. While, in the nightside, BEN consists of isolated, well-defined bursts (Pottelette et al., 1988) that are observed near the auroral kilometric radiation (AKR) sources, in the dayside it extends over a period of several minutes and many bursts can be observed during this period. A detailed analysis of BEN in the dayside auroral zone was presented by Dubouloz et al. (1991a). A large number of bursts of BEN were observed with frequencies ranging from lower hybrid and ion plasma frequencies up to, and sometimes well above electron plasma frequency. BEN emissions are associated with ion conical distributions and field-aligned electron beams. Most of the power is concentrated at low frequencies (lower hybrid and ion plasma frequencies) and high-frequency part may be associated with electron-acoustic and beam mode waves. During the recordings of two most intense bursts, upward and downward moving electron beams were observed alongwith isotropic hot electron population. Downward moving beam has 50 eV energy and upward moving beam has two components, one with $\leqslant$ 50–200 eV and other between 760 eV and 5.12 keV energy.

The $DE-1$ satellite provided the measurements of the particle and fields in Earth's polar region at 2–5 R_E. Observations showed electron beams moving in upward direction away from the Earth with energy ($\approx$100 eV) in the polar cusp region (Burch et al., 1983; Lin et al., 1984) and high-frequency field fluctuations known as hiss. Though, downward moving electron beams were also observed but they were of low intensity compared to upward moving electron beams. Lin et al. (1984) used $DE-1$ satellite data to study a correlation between electrostatic auroral hiss emissions at several kHz and upward moving electron beams at an altitude of 2–4R_E near the dayside polar cusp region. It is found that intense electrostatic hiss emissions at frequencies below the electron plasma frequency are associated with the upward moving electron beams. The wave frequencies with larger growth rates are found below the electron plasma frequency and are interpreted as electrostatic whistler waves propagating near the resonance cone. Later on, Tokar and Gary (1984) analyzed the full electromagnetic Vlasov dispersion equation of Lin et al. (1984) and studied the stability of the electrostatic and electromagnetic waves for the case of upward moving electron beams observed in the polar cusp region. Their numerical simulations clearly showed the whistler mode to be stable and electron-acoustic waves (EAWs) unstable. Thus, it was concluded that the upward moving electron beam can drive an electron-acoustic wave unstable rather than electrostatic whistlers near the resonance cone.

Electron acoustic modes travel at a speed greater than electron thermal speed and are important in space plasmas with two electrons (hot and cold) species. Watanabe and Taniuti (1977) used linear electrostatic Vlasov dispersion equation to show that electron acoustic waves can be destabilized in such a plasma. Later on, Yu and Shukla (1983) used fluid theory to obtain dispersion relation for EAWs in a two component electron–ion plasma with a condition $T_c/T_i \ll m_e/m_i$; where T_c and T_i are the temperatures of electron and ion, respectively. However, this condition is very difficult to satisfy. Gary and Tokar (1985) examined the electron acoustic modes using Vlasov theory in a three-component plasma with two Maxwellian electrons and thermal ions and obtained parameter regime for the propagation of these modes. Ashour-Abdalla and Okuda (1986) studied the electron-acoustic waves with four components cold and hot electrons, and thermal and beam ions. Both linear theory and simulations suggest that the instability contribute to the BEN in the geomagnetic tail. Bharuthram (1991) studied the theory of electron-acoustic instability driven by field-aligned hot electron beam in a three-component plasma. The electrons and ions are treated as magnetized and effect of temperature anisotropies of cold and hot electrons is also considered.

So far most studies on electron-acoustic waves have concentrated on three-component plasmas either with ion or electron beams with cold (hot) electron species and ions. However, observations have shown that the plasma in the Earth's magnetosphere consists of four species namely, cold electrons, hot electrons, beam electrons and ions. Motivated by the observations, we studied the generation of BEN by electron-acoustic waves in such a four component unmagnetized plasma. In this model, we considered cold and hot Maxwellian electrons, a drifting Maxwellian electron beam, and ions. We have generalized the previously existing three-component models (Gary and Tokar, 1985; Bharuthram, 1991) by including the hot electron component in addition to warm electron beam. Our model provides analytical results and thus, complements the numerical results of Tokar and Gary (1984). In the Section 2, dispersion relation for such a model is examined analytically for the real frequency and growth rate and the effect of various parameters such as beam drift speed, beam temperature and hot electron temperature on the instability were studied. In Section 3, results are applied to various regions of the Earth's magnetosphere, i.e., dayside auroral zone, polar cusp and magnetotail. It is found that highest frequency of the unstable electron acoustic waves can reach up to $\approx 0.45\omega_{pe}$ (where ω_{pe} is the total electron plasma frequency) in the polar cusp region.

2. Dispersion relation

We consider a homogeneous, unmagnetized plasma with four components, nondrifting cold and hot electrons with Maxwellian distribution, an electron beam drifting along the magnetic field and nondrifting ions. The dispersion relation for the electrostatic waves can be written as

$$1=\frac{1}{2k^2\lambda_{di}^2}Z'\left(\frac{\omega}{\sqrt{2}kv_i}\right)+\frac{1}{2k^2\lambda_{dc}^2}Z'\left(\frac{\omega}{\sqrt{2}kv_c}\right)+\frac{1}{2k^2\lambda_{dh}^2}Z'\left(\frac{\omega}{\sqrt{2}kv_h}\right)+\frac{1}{2k^2\lambda_{db}^2}Z'\left(\frac{\omega-kU_b}{\sqrt{2}kv_b}\right), \qquad (1)$$

where the subscripts, i, c, h and b represent ions, cold electrons, hot electrons and electron beam respectively; Z' is the derivative of the plasma dispersion function with respect to its argument, $v_j=\sqrt{T_j/m_j}$ ($j=$ i, c, h and b) is the thermal speed of the jth species; T_j and m_j are temperature and mass of the jth species; $\lambda_{dj}=v_j/\omega_{pj}$ (ω_{pj} is the plasma frequency) is the Debye length of the jth species and ω and k represents the frequency and wave number, respectively, and U_b is the electron beam drift speed. Electron-acoustic wave propagates at a phase speed satisfying the relation $v_c<\omega/k<v_h$. Under the approximations, $|\omega|\gg\sqrt{2}kv_i, \sqrt{2}kv_c$, $|\omega|\ll\sqrt{2}kv_h$ and $|(\omega-kU_b)|\leqslant\sqrt{2}kv_b$, the plasma dispersion function can be expanded to obtain the following simplified dispersion relation for the four-component plasma:

$$1+\frac{\omega_{ph}^2}{k^2v_h^2}+\frac{\omega_{pb}^2}{k^2v_b^2}-\left(\frac{\omega_{pc}^2+\omega_{pi}^2}{\omega^2}\right)+i\sqrt{\frac{\pi}{2}}\left[\frac{\omega\omega_{ph}^2}{k^3v_h^3}+\frac{(\omega-kU_b)\omega_{pb}^2}{k^3v_b^3}\exp\left\{-\frac{(\omega-kU_b)^2}{2k^2v_b^2}\right\}\right]=0. \qquad (2)$$

Solving the above dispersion relation for $\omega=\omega_r+i\gamma$, and considering $|\gamma|^2\ll|\omega_r|^2$, we get

$$\omega_r=k\lambda_{db}\sqrt{\frac{\omega_{pc}^2+\omega_{pi}^2}{1+k^2\lambda_{db}^2+\frac{n_hT_b}{n_bT_h}}} \qquad (3)$$

and

$$\gamma=-\sqrt{\frac{\pi}{8}}\sqrt{\frac{n_c/n_b+m_en_0/m_in_b}{(1+k^2\lambda_{db}^2+n_hT_b/n_bT_h)^{3/2}}}\left[\omega_r\left(\frac{n_h}{n_b}\right)\left(\frac{T_b}{T_h}\right)^{3/2}+(\omega_r-kU_b)\exp\left\{-\frac{(\omega_r-kU_b)^2}{2k^2v_b^2}\right\}\right]. \qquad (4)$$

In the limit $(\omega_r-kU_b)^2\ll 2k^2v_b^2$, Eq. (4) predicts unstable electron-acoustic waves, provided U_b exceeds a critical value given by

$$U_b>U_{cr}\approx\frac{v_b(n_c/n_b)^{1/2}[1+(n_h/n_b)(T_b/T_h)^{3/2}]}{(1+k^2\lambda_{db}^2+n_hT_b/n_bT_h)^{1/2}}. \qquad (5)$$

For $n_c/n_b \leqslant 1$, the U_{cr} can be quite low and the electron-acoustic instability can be easily excited. Also, it is interesting to see that U_{cr} increases with an increase of beam thermal speed v_b (or beam temperature T_b). Therefore an increase of beam electron temperature would tend to stabilize the mode.

3. Application

3.1. Auroral region BEN

First, we analyze the results in the light of auroral observations of broadband electrostatic noise that is a common phenomenon observed by the *Viking* satellite in the dayside auroral region at a height of 2000–10, 000 km. Frequency of the BEN is in the range from ion to electron plasma frequencies, sometimes even higher than electron plasma frequency. The Viking observations revealed that there exist downward as well as upward propagating electron beams with energies in the range $E_b\approx 50$ eV–5.12 keV and beam temperature $T_b\approx 50$ eV. Hot electron population has a thermal energy of about 250 eV and density around 2.5 cm^{-3}. The cold electron and beam densities are very low, $n_c<1$ cm^{-3} and $n_b\approx 1$ cm^{-3}, respectively. Here, we consider the cases of two most intense bursts namely, bursts *a* and *b* observed at 2030:20.191 UT and 2033:18.2015 UT (Viking Orbit 1188), respectively, in the auroral region (Dubouloz et al., 1991a, 1993). Burst *b* is more intense than burst *a*. Bursts *a* and *b* parameters are taken from Table 2 of Dubouloz et al. (1993); burst *a*: cold electron density $n_c=0.5$ cm^{-3}, hot electron density $n_h=2.0$ cm^{-3}, electron beam density $n_b=1$ cm^{-3}, cold electron temperature $T_c=2$ eV, hot electron temperature T_h=250 eV and electron beam temperature $T_b=50$ eV and burst *b*: $n_c=0.2$ cm^{-3}, $n_h=1.5$ cm^{-3}, and $n_b=1.0$ cm^{-3}. Other parameters are the same as for burst *a*.

The real frequency and growth rate can be easily computed from Eq. (3) and (4), respectively. Figs. 1a and b show the variation of normalized growth rate γ/ω_{pe} (ω_{pe} is the total electron plasma frequency) and real frequency (ω_r/ω_{pe}), respectively, with $k\lambda_{db}$ for the parameters of bursts *a* and *b* observed by *Viking* satellite (Dubouloz et al., 1991a, 1993), on the auroral field lines for various values of normalized electron beam speed U_b/v_b.

It can be seen from the Fig. 1a that as the beam speed increases the growth rate also increases. For the parameters of burst *a* the growth rate is maximum at normalized beam drift speed $U_b/v_b=1.4$ for $k\lambda_{db}\approx 0.9$ ($k\approx 2\times10^{-4}$ cm^{-1}). For $U_b/v_b>1.4$ the growth rate starts decreasing. The approximate real frequency (cf. Fig. 1b) of unstable EAWs

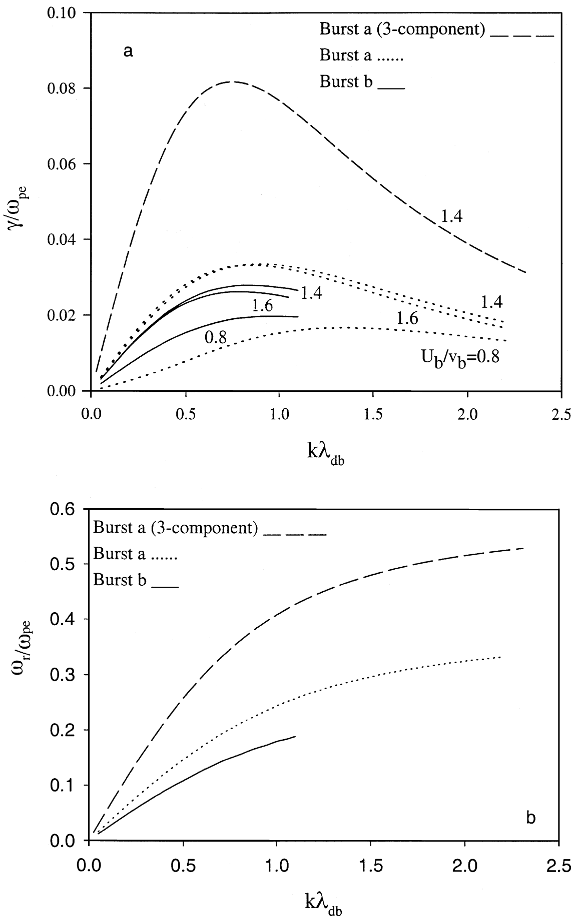

Fig. 1. (a) Normalized growth rate vs. $k\lambda_{db}$ for various values of beam drift speed for burst *a* and burst *b* parameters in dayside auroral region. Parameters for burst *a* are; $n_c = 0.5$ cm^{-3}, $n_h = 2.0$ cm^{-3}, $n_b = 1.0$ cm^{-3}, $T_c = 2$ eV, $T_h = 250$ eV, $T_b = 50$ eV and for burst *b*; $n_c = 0.2$ cm^{-3}, $n_h = 1.5$ cm^{-3}, $n_b = 1.0$ cm^{-3}, other parameters are the same as for burst *a*. The dashed curve (— — —) corresponds to three-component plasma (without hot electrons) for $U_b/v_b = 1.4$ for burst *a* parameters. (b) shows the variation of real frequencies corresponding to the parameters of Fig. 1(a). The dashed curve (— — —) corresponds to three-component plasma (without hot electrons) for $U_b/v_b = 1.4$ for burst *a* parameters.

corresponding to maximum growth rate is $\omega_r \approx 0.23\ \omega_{pe}$ which comes out to be about 4 kHz for $\omega_{pe}/2\pi \approx 17$ kHz. The frequency of unstable EAW is well above the ion plasma frequency of 400 Hz (for hydrogen ion plasma). In this region, the cold electron plasma frequency ($\omega_{pc}/2\pi$) is 6.4 kHz which is about 1.6 times higher than the EAW frequency. Further, the maximum frequency of electron-acoustic wave which can be excited through this model with a growth rate of about 300 Hz is about 5.6 kHz, very close to cold electron plasma frequency. If the BEN emissions are the result of cold electrons then we have good correspondence between the two frequencies. The maximum growth rate for linear EAW is 560 Hz that means the e-folding time for growth of these waves is about 2 ms; well below the few hundred milliseconds duration of these bursts. Thus, it can be emphasized here that linear EAWs in a four component plasma is a likely candidate to explain the BEN emissions in the auroral region. The frequency of unstable EAWs varies from 5 Hz to about 6 kHz for $T_h/T_c = 125$ (which is corresponding the to observed hot electron temperature $T_h = 250$ eV) and wave number $k \approx 2 \times 10^{-7} - 4 \times 10^{-4}$ cm^{-1} (cf. Fig. 1b).

For burst *b* parameters, the maximum growth rate occurs at U_b/v_b=1.4 and $k\lambda_{db}$=0.8 (k=1.5×10^{-4} cm^{-1}). The maximum value of growth rate is about 420 Hz and the corresponding frequency of EAW is 2.3 kHz which is about 15% of the total electron plasma frequency $\omega_{pe}/2\pi = 15$ kHz and about 57% of cold electron plasma frequency. The growth rate for EAWs is greater than the burst *a* case for $U_b/v_b \leqslant 1$ and vice versa. This implies that EAWs will be excited at a faster rate than burst *a* for $U_b/v_b \leqslant 1$. It is interesting to note that EAWs for burst *b* parameters can be excited only for $k\lambda_{db} \leqslant 1$, while for burst *a* parameters it can be excited for both short as well as long wavelengths. The frequency of unstable EAWs varies between 3 Hz and 3 kHz for $T_h/T_c = 125$ and $k = 2 \times 10^{-7}$–2×10^{-4} cm^{-1}. Thus, frequency of unstable EAWs is higher for burst *a* parameters than burst *b* and also, EAWs can be excited for larger range of frequencies. For burst *b* case, we have interrupted the curves because beyond $k\lambda_{db} \approx 1$ our assumptions is not satisfied. Also, in this figure and all subsequent figures we have plotted positive growth rates only and cutoff the curves where either of our assumptions is not satisfied. It may be remarked here that the frequency of unstable EAWs are in good agreement with the observed BEN emissions.

The growth rate and real frequency curves (— — —) at $U_b/v_b = 1.4$ have been plotted in Fig. 1a and b, respectively, for a three-component plasma consisting of cold electrons, warm electron beam and ions for burst *a* parameters to compare the results with four-component plasma. It is obvious from these figures that the growth rate and real frequency of the excited EAWs is much higher for three-component plasma than the four-component plasma.

Numerical results for burst *a* and *b* show that the increase in T_h/T_c value increases the growth rate of the instability (cf. Fig. 2a). This is expected as electron-acoustic instability occurs for $T_h/T_c \gg 1$ (also as seen from Eq. (4)). The corresponding real frequencies are plotted in Fig. 2b. It can be seen from Figs. 2a and b that the range of excited wave numbers for the burst *a* is larger compared to burst *b*. Also, we have plotted in Fig. 2b, one curve corresponding to the three-component plasma without the hot background electrons to compare the results with the four-component plasma. It is clearly seen that the waves with much higher frequency can be excited in three-component plasma.

The electric field spectral density for burst *a* peaks around 3–4 kHz (cf. Fig. 3 of Dubouloz et al., 1993), while our results show that the EAW frequency corresponding to maximum growth rate is about 4 kHz. For burst *b* parameters, the EAW frequency corresponding to maximum growth rate is about 2.3 kHz, while the observations show peak

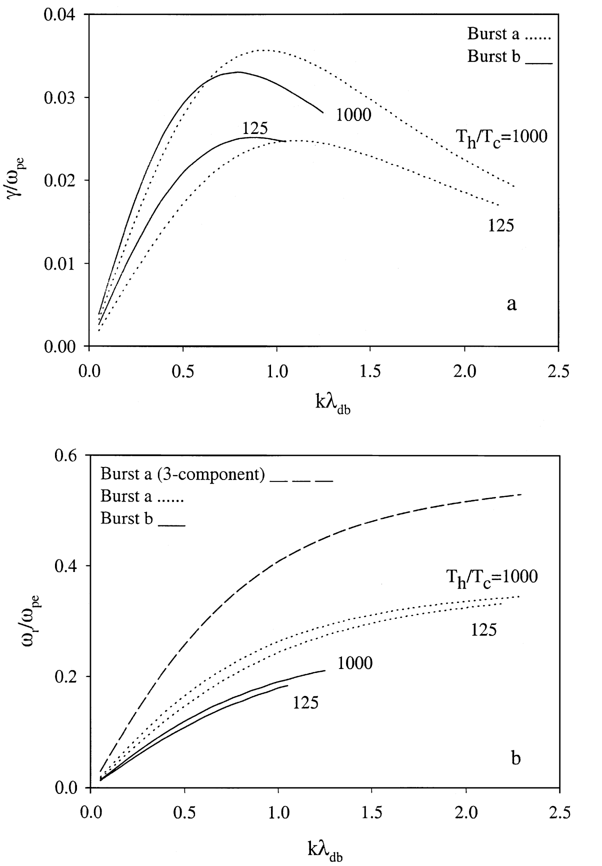

Fig. 2. (a) Normalized growth rate vs. $k\lambda_{db}$ for various values of T_h/T_c for $U_b/v_b = 1.0$ for burst *a* and burst *b* parameters. Other parameters are the same as for Fig. 1. (b) Normalized real frequency vs. $k\lambda_{db}$ for various values of T_h/T_c for burst *a* and burst *b* parameters of Fig. 1. The dashed curve (— — —) corresponds to three-component plasma (without hot electrons) for burst *a* parameters.

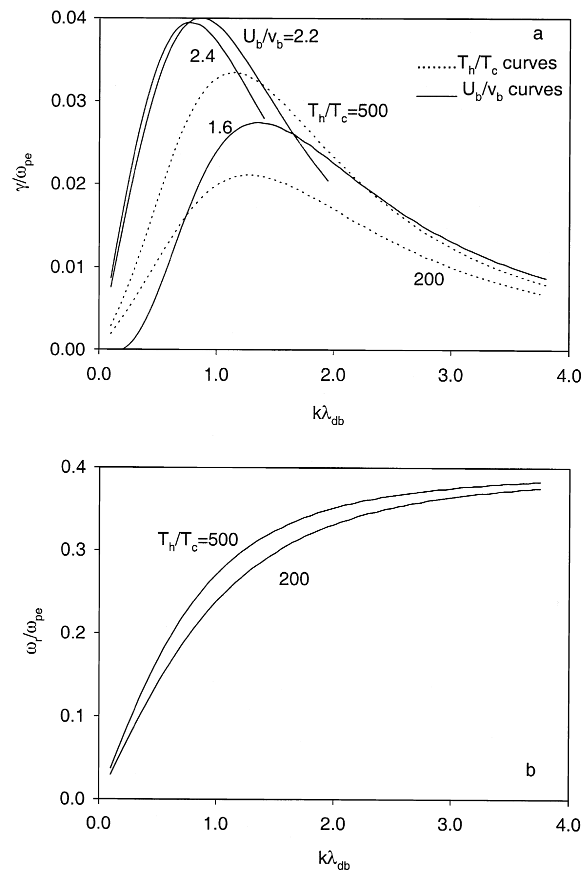

Fig. 3. (a) Normalized growth rate vs. $k\lambda_{db}$ for various values of beam drift speed and T_h/T_c for PSBL parameters; $n_c/n_h = 0.2$, $n_b/n_0 = 0.05$, $T_h/T_c = 500$, $T_b/T_c = 10$. Growth rate curves with T_h/T_c variation are plotted for $U_b/v_b = 1.8$. (b) shows the variation of normalized real frequency corresponding to different T_h/T_c values indicated on the respective curves.

electric field spectral density to be around 3 kHz (cf. Fig. 5 of Dubouloz et al., 1991a and Fig. 3 of Dubouloz et al., 1993). Thus, our results are in good agreement with the observations.

3.2. Plasma sheet boundary layer BEN

The observations from *ISEE* satellite have shown that the BEN emissions in this region have frequencies in the range 10 Hz–10 kHz. These BEN emissions can be generated by unstable electron distributions in the PSBL. For numerical computation purpose, the chosen parameters for the PSBL region are $n_b/n_0 = 0.05$, $n_c/n_h = 0.2$, $T_h/T_c = 500$, $T_b/T_c = 10$ (Parks et al., 1984 and Onsager et al., 1993). Figs. 3a and b shows the variation of normalized growth rate and real frequency, respectively, with normalized wave number for the above parameters for various beam drift speed and different hot to cold electron temperature ratio as indicated on the respective curves. The maximum growth rate is achieved at $U_b/v_b = 2.2$ for $k\lambda_{db} = 0.9$ ($k \approx 10^{-5}$ cm^{-1}). For $U_b/v_b > 2.2$ the growth rate decreases as can be seen from the Fig. 3a. Numerical results show that for drift speed $U_b/v_b < 1.6$, the instability grows only for $k\lambda_{db} \geqslant 1$. However, for higher drift speeds it can be driven unstable for large as well as small wave numbers. When beam temperature reaches the hot electron temperature, growth of electron-acoustic waves is not observed, a phenomenon common in the auroral as well as polar cusp regions. The probable reason for the stabilization is the increase of U_{cr} resulting in the violation of Eq. (5) when T_b/T_h is increased. The distinct feature of the results is that the instability demands larger value of electron beam drift speed as compared to auroral and polar cusp regions (cf. Fig. 3a).

Our results show that the frequency of EAW is about 2.5 kHz corresponding to the maximum growth rate of 400 Hz. The electron plasma frequency is taken to be 10 kHz. The maximum frequency of the EAW which can be excited here is about 3.8 kHz at $k\lambda_{db} \approx 4.4$ ($k \approx 5 \times 10^{-5}$ cm^{-1}). The frequency of unstable EAWs varies from 3 Hz to 4 kHz for $k = 10^{-8} - 5 \times 10^{-5}$cm^{-1} (cf. Fig. 3b), which is in good agreement of the observed frequencies in the PSBL.

Parks et al., (1984) have shown that n_b/n_0 varies from 0.005 to 0.05 in the PSBL region and in some cases it is up to 0.5. From numerical calculations, we observe that the increase in n_b/n_0 increases the growth rate of the instability. Thus, it is easier to excite EAWs with large n_b/n_0. This is a common feature in all the three regions discussed here. For very low electron beam density EAWs are stable as in such cases U_{cr} becomes very large (cf. Eq. (5)) and condition $U_b > U_{cr}$ is violated.

3.3. Polar cusp BEN

The chosen parameters for the polar cusp are $T_h = 86$ eV, $T_b = 20$ eV, $T_h/T_c = 1000$, $n_c = 0.5$ cm^{-3}, $n_h = 1.05$ cm^{-3} and $n_b = 0.85$ cm^{-3} (Lin et al., 1984). Here, it can be seen from Fig. 4a that as the beam speed increases, the growth rate increases and reaches a maximum value of 630 Hz at U_b/v_b=1.6 for $k\lambda_{db} \approx 0.85$ (k=2.4×10^{-4} cm^{-1}). For normalized speed larger than 1.6 the growth rate starts decreasing. For large k values, the growth rate decreases sharply and approaches zero. Also, the increase in beam speed restricts the instability to narrow range of wave numbers. The growth rate peaks are sharper than the auroral and PSBL regions. Also, growth rate for the polar cusp region is the largest of the other two regions and hence, EAWs can be excited faster. The frequency of unstable EAW is about 4 kHz corresponding to the maximum growth rate, that is 27% of the total electron plasma frequency in this region. However, if we compare the maximum frequency of EAW which is 6.3 kHz with the cold electron plasma frequency of 6.4 kHz, we have very good agreement between the two. The growth rate is large for the waves with frequencies well below the electron plasma frequency, which is in agreement with the observations (Lin et al., 1984). Also, the growth rate peaks are sharper and EAWs can be excited for wider range of wave numbers. We can excite EAWs with frequencies in the range 5 Hz to about 6 kHz for the wave number k varying from 3×10^{-7} to 2×10^{-3} cm^{-1} (cf. Fig. 4b). The observed hiss frequencies in the polar cusp region are in the range 4–10 kHz. Thus, the unstable frequency is well within the observed auroral hiss emission frequencies.

Figs. 4a and b also shows the damping and real frequency (dashed curves), respectively, for the three-component plasma of stationary cold and hot electrons and ions. We reproduce the real frequency curve of Tokar and Gary (1984) exactly. However, the damping curve is similar to theirs but the maximum damping in our case is somewhat smaller. This may be due to the fact that they solved a full electromagnetic dispersion relation where cold electrons and ions contribute to the damping. Our model does not take this into account.

Figs. 5a and b shows the variation of growth rate and real frequency, respectively, with normalized wave number for various T_h/T_b values as indicated on the curves. It can be seen from the Fig. 5a that the instability stabilizes when

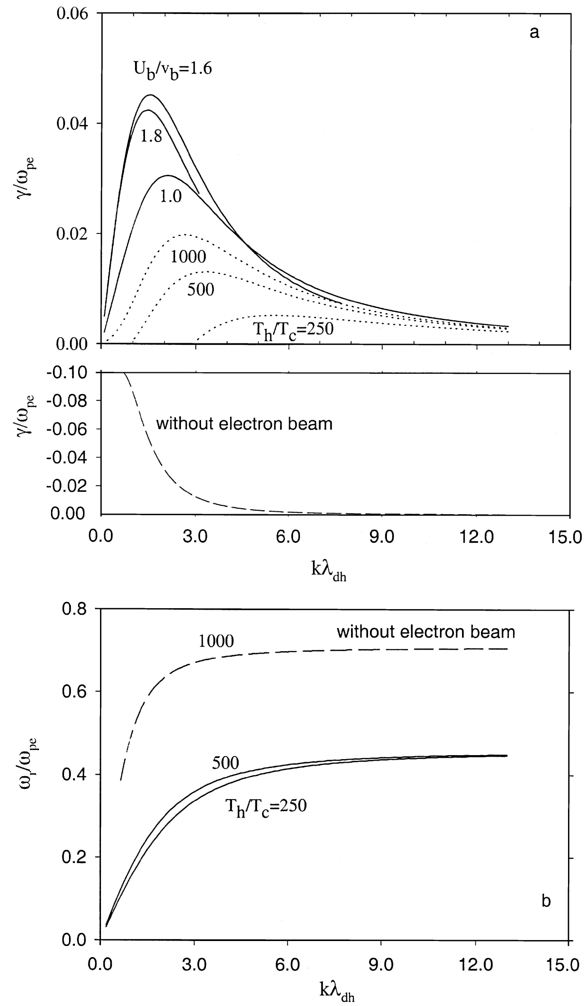

Fig. 4. (a) Normalized growth rate vs. $k\lambda_{dh}$ for various values of beam drift speed and T_h/T_c for polar cusp parameters; n_c=0.5 cm^{-3}, n_h=1.05 cm^{-3}, n_b=0.85 cm^{-3}, T_h=86 eV, T_b=20 eV, T_h/T_c = 1000. Growth rate curves with T_h/T_c variation are plotted for U_b/v_b = 1.6. The dashed (— — —) curve shows the damping in a three-component plasma without the electron beam. (b) shows the variation of real frequency for different T_h/T_c values indicated on the respective curves. The dashed (— — —) curve shows real frequency variation in a three-component plasma without the electron beam.

the electron beam temperature approaches the hot electron temperature. Also, the range of unstable wave number gets extended to large k values.

Now, we would like to discuss the implications of adding the hot electron component to the existing models of Gary and Tokar (1985) and Bharuthram (1991). In three-component model the frequencies of the excited EAWs are higher compared to the four-component model with hot background electrons and also growth of the wave is faster. The addition of the hot background electrons tends to reduce both the growth rate of the instability and the excited EAW frequencies as compared to the three-component model. The four-component model is more realistic and it can very well explain the BEN observations below the electron plasma frequencies. However, it cannot explain BEN

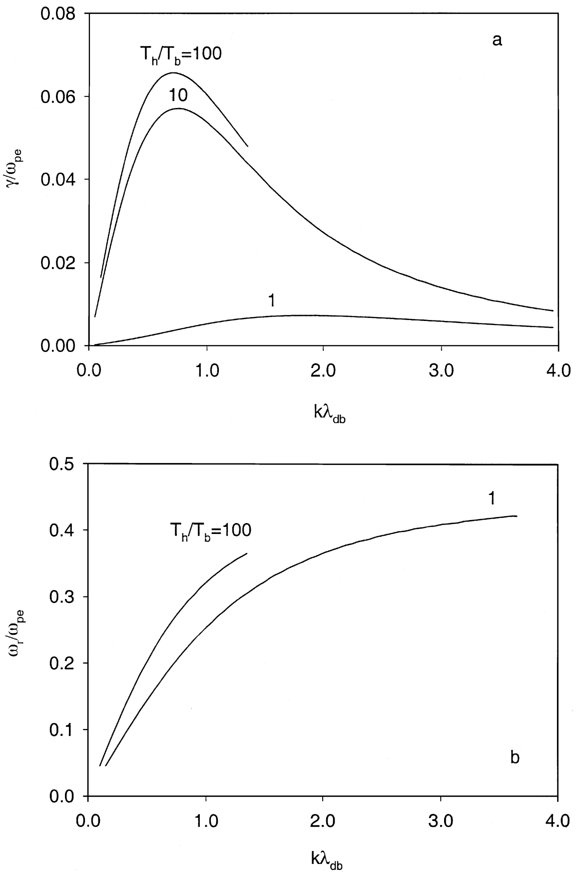

Fig. 5. (a) Normalized growth rate vs. $k\lambda_{\rm db}$ for various values of $T_{\rm h}/T_{\rm b}$ for $U_{\rm b}/v_{\rm b} = 1.6$. Other parameters are the same as for Fig. 4a. (b) shows the variation of real frequency for the parameters of the Fig. 4a.

observations with frequencies above total electron plasma frequencies, and thus, some alternate theories have to be developed in order to explain these observations.

4. Conclusions

The electron-acoustic wave model generalizes the existing three-component analysis of EAW to the case of four-component plasmas. The effect of adding hot electron component is found to be stabilizing. The system tends to stabilize when the electron beam temperature tends to hot electron temperature. Our analysis shows that the electron-acoustic waves can be generated by the electron beams in the dayside auroral region, polar cusp and plasma sheet boundary layer (PSBL). In the auroral region the real frequencies generated by EAW instability fall in the range ≈ 5 Hz–6 kHz, associated wavelength range is $\lambda = 2\pi/k \approx$ 160 m–314 km and with shorter wavelength corresponding to higher frequency. The maximum growth rate occurs at $\lambda \approx 370$ m. Similarly for the PSBL parameters, the mechanism predicts frequencies and wavelength of ≈ 3 Hz–4 kHz and 1–6300 km, respectively, and the maximum growth rate occurring at $\lambda \approx 7$ km. On the other hand, our mechanism can generate real frequencies ≈ 5 Hz to about 6 kHz with wavelength of 30 m–210 km for typical parameters of polar cusp region. The EAWs have maximum growth rate at $\lambda \approx 270$ m. The e-folding time of the instability in all the three regions is of the order of a few milliseconds.

Note that the growth rate of EAWs for all the regions is largest for frequencies well below the total electron plasma frequencies and $k\lambda_{\rm db} \leqslant 1$. The excited waves have higher frequencies at shorter wavelengths. The EAWs will have largest growth rate and real frequency in the polar cusp region. The addition of hot background electrons reduces the range of excited real frequencies and the growth rate. On the other hand, when the beam electron temperature approaches hot electron temperature, the growth rate reduces but the range of excited wave numbers increases. The detailed analysis of the problem in each region has shown, for the first time, that the growth rate attains a maximum at a certain value of electron beam velocity. It may be remarked here that waves with frequency close to cold electron plasma frequency can be excited by this model as computations revealed that the maximum frequency of unstable EAWs is close to cold electron plasma frequency. However, in order to explain BEN emissions with frequencies larger than total electron plasma frequency, some other mechanism has to be invoked.

We would like to point out that we have not considered the background magnetic field in our model. This is justified for the waves propagating parallel to the magnetic field as the effect of the magnetic field is significant for obliquely propagating waves. Since, we consider the waves to be propagating in the direction of the electron beams, our model would be applicable to the situations where the beams are directed along the magnetic field. We have also neglected the effect of density and magnetic field gradients in our model. Since, the gradients in density and magnetic field are important for obliquely propagating waves, we do not expect our results to change drastically for the case of parallel propagating waves. The linear theory predicts the wave generation by the observed distribution functions, and the growth rates are usually much smaller than the duration of the bursts. In a sense, these bursts of BEN are emissions averaged over many growth periods, and therefore represent saturated state of the waves. There can be nonlinear frequency shifts in the presence of large amplitude waves. What we have tried to show here is that the linear theory is capable of producing electrostatic waves in the observed frequency range of BEN.

The recent high-time resolution results on PSBL (Matsumoto et al., 1994) and auroral BEN (Ergun et al., 1998; Tsurutani et al., 1998 show that the noise consists of bipolar solitary pulses. These structures have been explained in terms of BGK-phase space electron holes produced by nonlinear two stream instability (Omura et al., 1994; Muschietti et al., 1999; Goldman et al., 1999). Since the EAWs can grow quickly, it is likely that they evolve nonlinearly into solitons as suggested by Dubouloz et al., (1991b, 1993).

Subsequently interaction of EAW solitary waves with ion-acoustic density fluctuations can lead to the modulated EAWs as observed by Pottelette et al. (1999). The nonlinear EAW structure may give rise to significant heating and acceleration of the charged particles.

References

Akimoto, K., Omidi, N., 1986. Geophys. Res. Lett. 13, 97.
Ashour-Abdalla, M., Okuda, H., 1986. Geophys. Res. Lett. 13, 366.
Baumjohann, W., Treumann, R.A., Labelle, J., Anderson, R.R., 1989. J. Geophys. Res. 94, 15221.
Bharuthram, R., 1991. J. Plasma Phys. 46, 1.
Burch, J.L., Reifff, P.H., Sugiura, M., 1983. Geophys. Res. Lett. 10, 753.
Cattell, C.A., Mozer, F.S., Anderson, R.R., Hones Jr., E.W., Sharp, R.D., 1986. J. Geophys. Res. 91, 5688.
Dubouloz, N., Pottelette, R., Malingre, M., Holmgren, G., Lindqvist, P.A., 1991a. J. Geophys. Res. 96, 3565.
Dubouloz, N., Pottelette, R., Malingre Treumann, R.A., 1991b. Geophys. Res. Lett. 18, 155.
Dubouloz, N., Treumann, R.A., Pottelette, R., Malingre, M., 1993. J. Geophys. Res. 98, 17415.
Ergun, R.E., et al., 1998. Geophys. Res. Lett. 25, 2041.
Gary, S.P., Tokar, R.L., 1985. Phys. Fluids. 28, 2439.
Goldman, M.V., Oppenheim, M.M., Newman, D.L., 1999. Geophys. Res. Lett. 26, 1821.
Grabbe, C.L., 1985. Geophys. Res. Lett. 12, 483.
Grabbe, C.L., Eastman, T.E., 1984. J. Geophys. Res. 89, 3865.
Gurnett, D.A., Frank, L.A., 1977. J. Geophys. Res. 82, 1031.
Gurnett, D.A., Frank, L.A., Lepping, R.P., 1976. J. Geophys. Res. 81, 6059.
Hada, T., Nishida, A., Terasawa, T., 1981. J. Geophys. Res. 86, 11211.
Heppner, J.P., 1969. In: B.M. McCormac, A. Omholt (Eds.), Atmospheric Emissions, Reihold, New York, p. 251.
Huba, J.D., Gladd, N.T., Papadopoulos, K., 1978. J. Geophys. Res. 83, 5217.
Lakhina, G.S., 1987. J. Geophys. Res. 92, 12161.
Lin, C.S., Burch, J.L., Shawhan, S.D., Gurrnett, D.A., 1984. J. Geophys. Res. 89, 925.
Matsumoto, H., Kojima, H., Miyatake, T., Omura, Y., Okada, M., Tsutsui, M., 1994. Geophys. Res. Lett. 21, 2915.
Muschietti, L., Ergun, R.E., Roth, I., Carlson, C.W., 1999. Geophys. Res. Lett. 26, 1093.
Omidi, N., 1985. J. Geophys. Res. 90, 12330.
Omura, Y., Kojima, H., Matsumoto, H., 1994. Geophys. Res. Lett. 21, 2923.
Onsager, T.G., Thomsen, M.F., Gosling, J.T., Bame, S.J., 1990. Geophys. Res. Lett. 17, 1837.
Onsager, T.G., Thomsen, M.F., Elphic, R.C., Gosling, J.T., Anderson, R.R., Kettmann, G., 1993. J. Geophys. Res. 98, 15509.
Parks, G.K., et al., 1984. J. Geophys. Res. 89, 8885.
Pottelette, R., Malingre, M., Bahnsen, A., Eliasson, L., Stasiewicz, K., Erlandson, R.E., Marklund, G., 1988. Ann. Geophys. 6, 573.
Pottelette, R., Ergun, R.E., Treumann, R.A., Berthomier, M., Carlson, C.W., McFadden, J.P., Roth, I., 1999. Geophys. Res. Lett. 26, 2629.
Scarf, F., Frank, L., Ackerson, K., Lepping, R., 1974. Geophys. Res. Lett. 1, 189.
Shriver, D., Ashour-Abdalla, M., 1987. J. Geophys. Res. 92, 5807.
Shriver, D., Ashour-Abdalla, M., 1989. Geophys. Res. Lett. 16, 899.
Tokar, R.L., Gary, S.P., 1984. Geophys. Res. Lett. 11, 1180.
Tsurutani, B.T., Arballo, J.K., Lakhina, G.S., Ho, C.M., Buh. B., Pickett, J.S., Gurnett, D.A., 1998. Geophys. Res. Lett. 25, 4117.
Watanabe, K., Taniuti, T., 1977. J. Phys. Soc. Jpn. 43, 1819.
Yu, M.Y., Shukla, P.K., 1983. J. Plasma Phys. 29, 1409.